

Electronic structure and X-ray magnetic circular dichroism of CrO₂

V. Kanchana and G. Vaitheeswaran

Max-Planck-Institut für Festkörperforschung, Heisenbergstrasse 1, 70569 Stuttgart, Germany

M. Alouani

*Institut de Physique et de Chimie des Matériaux de Strasbourg (IPCMS),
23 rue du Loess, 67037 Strasbourg Cedex, France*

(Dated: September 7, 2021)

A detailed theoretical study on the electronic structure and magnetic properties of half-metallic ferromagnet CrO₂ was carried out by means of relativistic full-potential linear muffin-tin orbital method within the generalized gradient approximation (GGA) to the exchange correlation potential. Our calculation favours the [001] magnetization axis to be the easy axis of magnetization when compared to the [100] axis which is in agreement with the experiments. The calculated spin and orbital magnetic moments of Cr agrees well with the experimental and other theoretical works. The Cr L_{2,3} x-ray absorption and x-ray magnetic circular dichroism (XMCD) spectra were calculated for both the quantization axis and compared with the experiment. In addition the oxygen K edge and XMCD spectra were also calculated which compares well with the experiments. The XMCD sum rules were used to compute the spin and orbital magnetic moments and results agree quite well with the direct calculation.

PACS numbers: 75.50.Ss, 71.20.Lp, 75.30.Et

I. INTRODUCTION

Chromium dioxide is the only stoichiometric binary oxide that is a ferromagnetic metal and also is the simplest and best studied half metal¹. In recent years, magneto electronic devices such as spin valve field sensors and magnetic random access memories have emerged, where both charge and spin of electrons are exploited using spin-polarized currents and spin-dependent conduction^{2,3}. The performance of such magneto-electronic devices depends critically on the substantial spin polarization of the ferromagnetic components. CrO₂ attracts specific interest being the only compound reported so far experimentally to possess 100% spin polarization. The half-metallic band structure of CrO₂ was confirmed by several experimental techniques such as Andreev reflection, superconducting tunnelling, photoemission, point-contact magnetoresistance, x-ray absorption, resonant scattering and Raman spectroscopy^{4,5,6,7,8,9,10,11,12,13}.

Half-metallic ferromagnetic materials appear as potential candidates and a lot of work is under progress to synthesis magnetic oxides such as CrO₂, Fe₃O₄ and Sr₂FeMoO₆ which are found to possess high Curie temperature (T_c). Recently Sr₂CrReO₆ a Cr based double perovskite is found to have a largest T_c of about 635 K which is the highest among the double perovskite family¹⁴. These compounds serve as perspective materials in the field of spintronics¹⁵. Numerous theoretical works are available for CrO₂ explaining the electronic structure, bonding, optical and magneto-optical properties and magneto-crystalline anisotropy (MCA) etc^{16,17,18,19,20,21,22,23,24,25}. Because of the uniaxial crystal structure, CrO₂ is expected to have a large magnetic anisotropy which makes it the favoured material for

magneto-optical recording. Recently it has been shown that the low-temperature experimental data were reproduced well by LSDA itself without taking into account the Hubbard *U* correction confirming that the ordered phase of CrO₂ is weakly correlated²⁵.

The circular dichroism-type spectroscopy became a powerful tool in the study of the electronic structure of magnetic materials^{26,27}. It has been recently demonstrated by Weller et al²⁸ that x-ray magnetic circular dichroism (XMCD) is also a suitable technique to probe MCA at an atomic scale, via the determination of anisotropy of the orbital magnetic moment on a specific shell and site. The x-ray absorption spectroscopy (XAS) using polarized radiation probes element specific magnetic properties of compounds via the XMCD by applying the sum rules to the experimental spectra^{29,30,31}. The application of these sum rules to itinerant systems, in particular to low symmetry systems, is debated since the sum rules are derived from atomic theory^{30,32,33}. Recently angle resolved XMCD technique has been applied by Georing et al^{34,35,36} for a wide range of temperature to investigate the anisotropies of orbital moments l_z and magnetic dipole term t_z of Cr atom in epitaxial CrO₂ films on TiO₂ substrate. From their XMCD studies they found large anisotropies of l_z and t_z , where the latter was derived from the semi empirical van der Laan's method of moment analysis³⁷.

Theoretical understanding of XMCD for magnetic material is not an easy task, and several *ab initio* calculations have attempted to compute XMCD of transition metals and rare-earth compounds^{33,38,39,40,41,42,43,44}. The L₂ and L₃ edges involving electronic excitations of the 2*p*-core electrons towards *d*-conduction states have attracted much attention due to the dependence of the

XMCD spectra on the exchange-splitting and the spin-orbit coupling of both initial core and final conduction states. Brouder and co-workers⁴⁰, Guo⁴¹, and Ankudinov and Rehr⁴² used multiple-scattering theory to study XMCD but their method, although successful, has been applied to systems with few atoms per unit cell, as their formalism is computationally involved. Finally, atomic calculations, using crystal-field symmetry, were widely applied to fit the experimental $M_{4,5}$ edges of the rare earths and actinide compounds and the $L_{2,3}$ edges of early transition metals. Because of the large number of parameters to fit, it is difficult to apply this formalism to delocalized $3d$ states⁴⁵. Though there are lot of theoretical studies available explaining the electronic and magnetic properties of CrO_2 theoretical studies on the XMCD spectra were not available. Parallel to our study, Baadji and coworkers⁴⁶ are investigating the effect of Hubbard interaction on the magnetic properties and XMCD spectra of CrO_2 using the linear Augmented plane wave method.

In the present study, efforts were taken to study theoretically the $L_{2,3}$ edge of Cr and K-edge of oxygen of CrO_2 using relativistic full-potential linear muffin-tin orbital method (FP-LMTO) method. In Section II we briefly present the theoretical method used to calculate the electronic structure, orbital magnetic moment and XMCD spectra. The density of states and magnetic moments are discussed in Section III. In Section IV we calculate the XAS and XMCD spectra of CrO_2 and compare with the experiment. The conclusion of the results are presented in Section V.

II. THEORETICAL DETAILS

In the present work electronic structure calculations were performed using the all-electron full-potential linear muffin-tin orbital (FP-LMTO) method⁴⁷ including the spin-orbit interaction directly in the Hamiltonian. The exchange correlation potential is parametrized using the generalized gradient approximation (GGA)⁴⁹. In this method, space is divided into non-overlapping muffin-tin spheres surrounding the atoms, and an interstitial region. Most importantly, this method assumes no shape approximation of the potential, wave functions, or charge density. The spherical-harmonic expansion of the potential was performed up to $l_{max} = 6$, and we used a double basis so that each orbital is described using two different kinetic energies in the interstitial region. The basis set consisted of the Cr ($4s$ $4p$ $3d$), O ($2s$ $2p$) LMTOs. We performed our calculations using the experimentally determined structure and atomic positions, i.e., the rutile structure with space group symmetry $P4_2/mmm$ and with cell parameters $a = b = 4.419 \text{ \AA}$, $c = 2.912 \text{ \AA}$ ⁵⁰. The radii of the muffin-tin spheres used for Cr and O were 2.0 and 1.5 Bohr units respectively. To find the easy magnetization axis we calculated total energy only for [001] as well as [100] magnetization axis. The integration

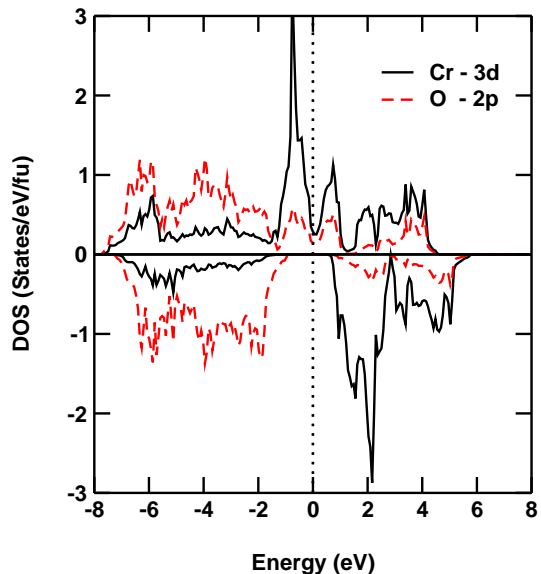


FIG. 1: (Color online) Calculated partial Cr-3d and O-2p density of states of CrO_2 the dotted line represents the Fermi level

in reciprocal space was performed using the tetrahedron method⁴⁸ and 1100 irreducible \mathbf{k} points in the Brillouin zone (BZ), for the [001] magnetization axis, whereas for [100] magnetization axis 1200 \mathbf{k} points were used using the same BZ grid as for the previous quantization axis. To avoid numerical errors one has to use the same \mathbf{k} grid for both spin quantization axis and let the symmetry of the crystal in presence of the spin-orbit decide for the number of irreducible \mathbf{k} points. The theoretical XAS and XMCD spectra was calculated using the method described elsewhere³⁹. This method was found to be successful in reproducing the experimental XAS and XMCD spectra of several transition metal compounds^{39,43,44}.

III. DENSITY OF STATES AND MAGNETIC MOMENTS

The electronic structure of CrO_2 has been extensively reported in the literature^{16,17,18,19,20,21,22,23,25} so in this section we briefly discuss the density of states and compare with the earlier works.

Figure 1 shows the density of states (spin up and down) of Cr-3d and O-2p states. For the majority spin, the Fermi level lies near a local minimum of the Cr $3d-t_{2g}$ band with the DOS at the Fermi level. For the minority spin, the Fermi level falls in a gap of 1.34 eV which is in agreement with the earlier results^{16,19,20,21,22}. The calculated exchange splitting between the majority and the minority spin main peaks of the Cr $3d-t_{2g}$ band is found to be 2.3 eV. A similar splitting of 2.5 eV has been found in FPLAPW calculations²¹, while a splitting of 2.3 eV has been found in a recent FPLMTO calculations²².

All the exchange splitting calculated within the LSDA or GGA are too small when compared with the measured large splitting of about 5 eV between the main peaks in the occupied and the empty Cr-3d DOS, from experimental photoemission studies⁵¹. It is interesting to note that half-metallic gap persists even with spin-orbit coupling. In general the spin-orbit coupling eventually destroys the half-metallic nature in many Huesler alloys, dilute magnetic semiconductors, zinc blende type transition metal pnictides and double perovskites^{52,53}.

The calculated spin and orbital magnetic moments along the [001] axis of magnetisation are found to be $1.99 \mu_B$ and $-0.045 \mu_B$ /atom for Cr and $-0.08 \mu_B$ and $-0.0017 \mu_B$ /atom for O respectively. The calculated spin magnetic moments of Cr and O are slightly higher when compared to the recent FP-LMTO calculations of Jeng and Guo²² within the LSDA. In the present calculation we have used GGA to the exchange correlation which will tend to increase the magnitude of the spin moment. When comparing the orbital magnetic moments of Cr and O they compares well with the recent FLAPW calculations²⁴. From the above results it can be seen that the the orbital magnetic moment of Cr is almost quenched and is also antiparallel to the spin moment, which is consistent with Hund's rule for 3d shells which are less than half-filled. A similar quenched orbital magnetic moment for Cr has been recently reported in the double perovskite $\text{Sr}_2\text{CrReO}_6$ ⁵³. The orbital magnetic moment of the O atom is parallel to the spin moment because the O-2p shell is more than half-filled. The calculated spin moment of oxygen is antiparallel to the spin moment of Cr and hence the Cr and O are coupled antiferromagnetically. The calculated orbital magnetic moments of Cr and O are found to be -0.045 and $-0.0017 \mu_B$ /atom respectively which are slightly lower when compared with the experimental XMCD measurements of Huang et al in which they obtained a value of $-0.06 \pm 0.02 \mu_B$ /Cr and $-0.003 \pm 0.001 \mu_B$ /O respectively in the [001] axis of magnetization⁵⁴. While Georing et al³⁴ in their XMCD measurements on CrO_2 films found a relatively small contribution to the orbital magnetic moment of Cr in the [001] axis of magnetization which is found to be $-0.02 \mu_B$. When comparing the true spin moment of Cr atom Georing et al³⁴ obtained a value of $1.2 \mu_B$. In order to explain the magnetic moment of $2 \mu_B$ per unit cell which was obtained from the superconducting quantum interference device (SQUID) measurements the above authors assumed a very large spin moment of about $0.4 \mu_B$ per O which they try to explain in terms of hybridization between the Cr and oxygen. Recently the same authors applied spin correction factor to their spectra from which they were able to get a spin magnetic moment of $2.4 \mu_B$ which is slightly higher when compared to the present theoretical and other experimental works⁵⁵. For the oxygen atom the spin moments are once again too low when compared to the value estimated by Georing et al³⁴. However it was recently shown by Komelj et al²⁴ that calculations with Hubbard $U = 3$ eV yield

TABLE I: Spin and orbital magnetic moments as determined from sum rules(SR) and self-consistently (SC) of Cr-d along the [001] axis of magnetization along with the experimental values ^aReference⁵⁴, ^bReference³⁴, ^cReference⁵⁵

μ_s		μ_l		Expt.	
SR	SC	SR	SC	μ_s	μ_l
1.82	1.99	-0.044	-0.045	1.9 ± 0.1^a	-0.06 ± 0.02^a
				1.2^b	-0.02^b
				2.15^c	

a spin moment of $0.1 \mu_B$ which is a factor of 4 times smaller than the value obtained by Georing et al³⁴. In order to find the easy axis of magnetization we have done self consistent calculations only along the [001] and [100] magnetization axis. Our calculations find [001] axis to be the easy axis of magnetization which is in agreement with the experiments^{36,56,57,58,59}.

IV. X-RAY ABSORPTION AND MAGNETIC CIRCULAR DICHROISM

In this section we calculate, analyse and compare the XMCD spectra with experiment. At the core level edge XMCD is not only element specific but also orbital specific. For 3d transition metals, the electronic states can be probed by the K, $L_{2,3}$, $M_{2,3}$ x-ray absorption and emission spectra. The dichroism at the L_2 and L_3 edges is influenced by the spin-orbit coupling of the initial 2p core states. The large SO splitting of the core levels gives rise to a very pronounced dichroism in comparison with the dichroism at the K-edge. In figure 2, we present the XAS and XMCD spectra for Cr atom in the [001] axis of magnetization. We convoluted our theoretical spectra using a Lorentzian and Gaussian width of 0.5 eV. The Gaussian represents the experimental resolution while Lorentzian corresponds to the width of the core hole.

The calculated total absorption spectra corresponding of the Cr $L_{2,3}$ edge was shown in the upper part (figure 2). We have scaled our spectra in a way that the experimental and theoretical L_3 peaks in the absorption spectra have the same intensity. The energy difference between the L_3 and L_2 peaks is given by the spin-orbit splitting of $p_{1/2}$ and $p_{3/2}$ core states which is 8.65 eV. The calculated value agrees well with the experimental value of 8.2-8.6 eV⁵⁵. As far the absorption spectra is concerned the present theory represents well the experimental features but underestimates the intensity of the L_2 peak.

The intensity of the L_3 edge in the x-ray absorption spectra when compared to the L_2 peak is a bit high which is in agreement with the experiment. The calculated XMCD spectra along the [001] axis of magnetization is shown in the lower part. The present calculations reproduce well the shape of the experimental spectra.

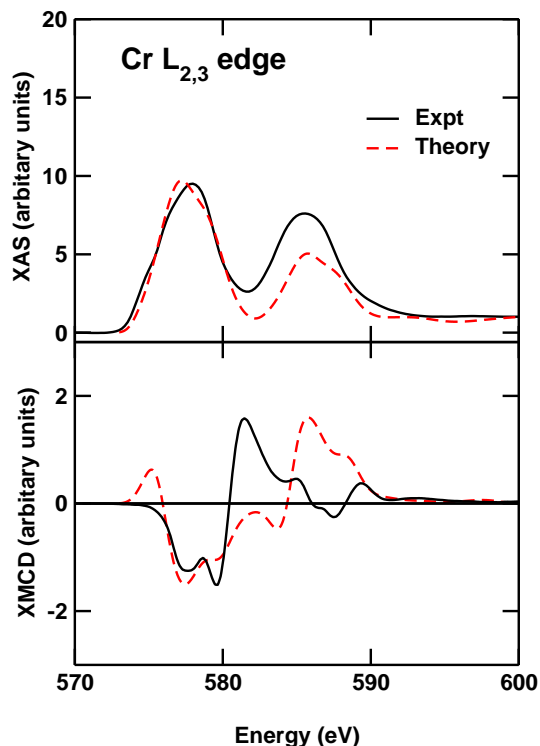


FIG. 2: (Color online) Cr $L_{2,3}$ XAS and XMCD spectra of CrO₂ along the [001] magnetisation axis. The experimental spectra is taken from Ref.34

Using the XMCD sum rules we calculate the spin and orbital magnetic moment of Cr-3d state which are found to be 1.82 and $-0.044 \mu_B/\text{atom}$ respectively and these values of spin and orbital magnetic moments are in agreement with the values obtained from the self-consistent calculations. A deviation of about 10% in the magnetic moments when comparing the values from sum rules and direct calculation may result from the spectral overlap⁶⁰. When comparing the spin and orbital magnetic moments obtained using the sum rules with the theoretical LSDA values of Huang et al⁵⁴ the spin moment of Cr is slight lower when compare to the theoretical value of $1.9 \pm 0.1 \mu_B$ whereas the orbital magnetic is found to be $-0.06 \pm 0.02 \mu_B$ which is in good agreement with the present calculations. However the experimental studies of Huang et al⁵⁴ could not provide quantitative information on the spin moment of Cr, because they cannot uniquely define which part of spectra belongs to the L_3 or L_2 edge. When comparing our magnetic moments obtained from sum rules with that of the XMCD measurements of Georing³⁴ the spin magnetic moment are too low ($1.2 \mu_B$), whereas the spin magnetic moment ($2.4 \mu_B$) obtained by the same authors after spin correction applied to the spectra⁵⁵ is slightly higher when compared to the present calculations. The orbital magnetic moments are also slightly higher ($-0.044 \mu_B$) when compared to the experimental results of Georing in which they obtain a

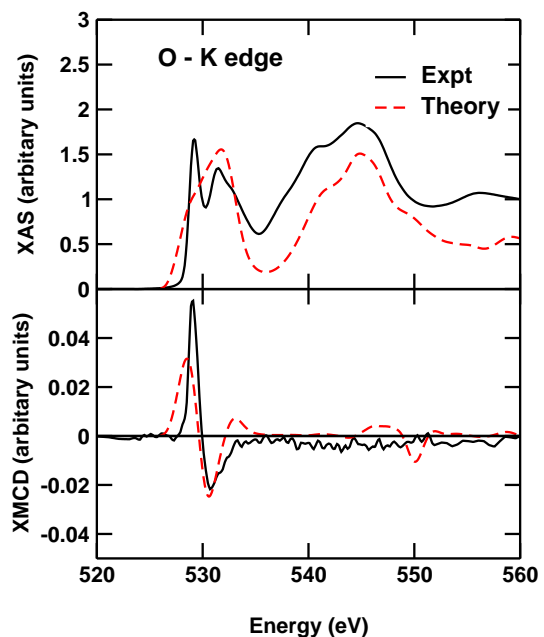


FIG. 3: (Color online) O K-edge XAS and XMCD spectra of CrO₂ along the [001] magnetisation axis. The experimental spectra is taken from Ref.35

value of $-0.02 \mu_B$.

In figure 3, we have shown the oxygen K edge XAS and XMCD spectra along the [001] axis of magnetization.

We used a similar broadening as that of the Cr $L_{2,3}$ for the oxygen K edge. The oxygen K edge spectrum mainly comes from excitation of the 1s state and is less intense when compared to the $L_{2,3}$ edge of Cr. The exchange splitting of the initial 1s core state is extremely small value, therefore, only the exchange and spin-orbit splitting of the final 2p state is responsible for the observed dichroism at the K-edge. However the present calculation reproduce fairly well the experimentally observed O-K edge and XMCD spectra.

In figure 4, the Cr $L_{2,3}$ XAS and XMCD spectra of CrO₂ along the [100] axis of magnetization is also shown.

The core level splitting of 8.6 eV is found in this axis which is in agreement with experimental value of 8.2-8.6⁵⁵. The theoretical XAS spectra agrees quite well with the experiments except the intensity of the L_2 peak is lower when compared to the experiment. The calculated XMCD spectra is shown in the lower part reproduce well the shape of the experimentally observed features. The calculated XMCD intensity is relatively less in the [100] magnetization axis when compared to the [001] axis of magnetization. For both the axes, the low intensity of the calculated L_2 edge makes the theoretical XMCD integrated L_3/L_2 branching ratio to be much larger than the experimental one. This discrepancy may be due to the negligence of 3d core-hole interaction. Using the XMCD sum rules the spin and orbital magnetic moments of Cr atom along the [100] magnetization axis is found

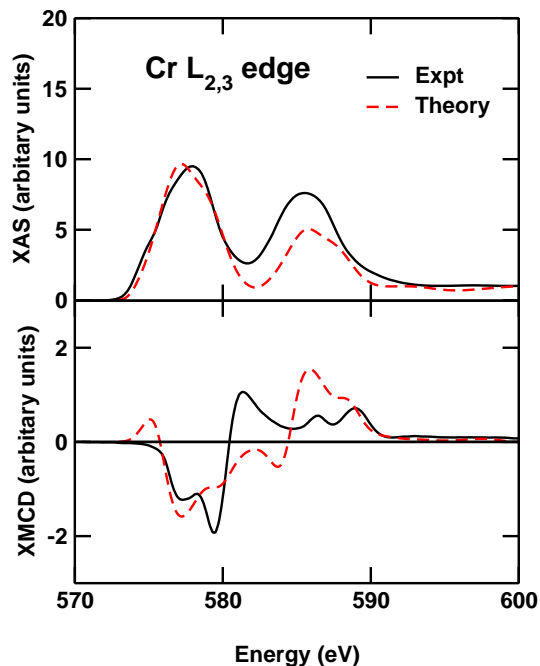


FIG. 4: (Color online) Cr $L_{2,3}$ XAS and XMCD spectra of CrO_2 along the $[100]$ magnetisation axis. The experimental spectra is taken from Ref.34

to be $1.844 \mu_B$ and $-0.004 \mu_B$, respectively. The calculated spin magnetic moment agrees well with the earlier calculations^{22,24}. The orbital magnetic moment obtained from the sum rules in the $[100]$ axis is much lower when compared to the direct calculations. A similar discrepancy was observed in NiMnSb in which the orbital mag-

netic moments of Mn obtained from sum rules are much lower when compared to the direct calculation⁴³. However the theoretical orbital magnetic moments are much lower when compared to the experimental values of $-0.09 \mu_B$ ³⁴.

The oxygen orbital magnetic moment is almost quenched in the $[100]$ axis, which are similar to the earlier theoretical works^{22,24} resulting in a weak intensity of the oxygen K edge in contrast to the experiments, which show the same angular dependency for the Cr- $3d$ orbital projections and the O-K edge XMCD.

V. CONCLUSIONS

In the present work we have carried out a detailed theoretical study on the magnetic properties of CrO_2 . The calculated half-metallic band structure of CrO_2 is in agreement with earlier studies. Our calculation confirms the c -axis to be the easy axis of magnetisation. The calculated XAS and XMCD spectra of Cr $L_{2,3}$ and oxygen K edge compares fairly well with the experimental results. The L_3/L_2 branching ratio is higher when compared to the experiments which could be improved by including the $3d$ core-hole interaction. In addition the spin and orbital magnetic moments obtained from the sum rules are compared with the direct calculations.

Acknowledgments

The authors acknowledge Dr. E. Goering for sharing experimental details. M.A. thanks O.K. Andersen for an invitation to the MPI during the completion of this work.

- ¹ J. M. D. Coey, and M. Venkatesan, *J. Appl. Phys.* **91**, 8345 (2002).
- ² G. A. Prinz, *Phys. Today*, **48**, 58 (1995).
- ³ J. M. Daughton, A. V. Pohm, R. T. Fayfield, and C. H. Smith, *J. Phys. D* **32**, R169 (1999).
- ⁴ Y. Ji, G. J. Strijkers, F. Y. Yang, C. L. Chein, J. M. Byers, A. Anguelouch, G. Xiao, and A. Gupta, *Phys. Rev. Lett.* **86**, 5585 (2001).
- ⁵ J. S. Parker, S. M. Watts, P. G. Ivanov, and P. Xiong, *Phys. Rev. Lett.* **89**, 196601 (2001).
- ⁶ K. P. Kämper, W. Schmitt, G. Güntherodt, R. J. Gambino, and R. Ruf, *Phys. Rev. Lett.* **59**, 2788 (1987).
- ⁷ Y. S. Dedkov, M. Fonine, C. Konig, U. Rudiger, G. Güntherodt, S. Senz, and D. Hesse, *Appl. Phys. Lett.* **80**, 4181 (2002).
- ⁸ J. M. D. Coey, A. E. Berkowitz, L. I. Balcells, F. F. Putris, and A. Barry, *Phys. Rev. Lett.* **80**, 3815 (1998).
- ⁹ J. M. D. Coey, and S. Sanvito, *J. Phys. D* **37**, 988 (2004).
- ¹⁰ D. J. Huang, L. H. Tjeng, J. Chen, C. F. Chang, W. P. Wu, S. C. Chung, A. Tanaka, G. Y. Guo, H.-J. Lin, S. G. Shyu, C. C. Wu, and C. T. Chen, *Phys. Rev. B* **67**, 214419 (2003).
- ¹¹ C. B. Stagarescu, X. Su, D. E. Eastman, K. N. Altmann, F. J. Himpsel, A. Gupta, *Phys. Rev. B* **61**, R9233 (2000).
- ¹² E. Z. Kurmaev, A. Moewes, S. M. Butorin, M. I. Katsnelson, L. D. Finkelstein, J. Nordgren, and P. M. Tedrow, *Phys. Rev. B* **67**, 155105 (2003).
- ¹³ M. N. Iliev, A. P. Litvinchuk, H.-G. Lee, C. W. Chu, A. Barry, and J. M. D. Coey, *Phys. Rev. B* **60**, 33 (1999).
- ¹⁴ H. Kato, T. Okuda, Y. Okimoto, Y. Tomioka, Y. Takenoya, A. Ohkubo, M. Kawasaki and Y. Tokura, *Appl. Phys. Lett.* **81**, 328 (2002).
- ¹⁵ A. M. Haghiri-Gosnet, T. Arnal, R. Soulimane, M. Koubaa, and J. P. Renard, *Physica Status Solidi (a)* **201**, 1392 (2004).
- ¹⁶ K. Schwarz, *J. Phys. F* **16**, L211 (1986).
- ¹⁷ P. I. Sorantin, and K. Schwarz, *Inorg. Chem.* **31**, 567 (1992).
- ¹⁸ Yu. A. Uspenskii, E. T. Kulatov, and S. V. Halilov, *Phys. Rev. B* **54**, 474 (1996).
- ¹⁹ S. P. Lewis, P. B. Allen, T. Sasaki, *Phys. Rev. B* **55**, 10253 (1997).
- ²⁰ M. A. Korotin, V. I. Anisimov, D. I. Khomskii, and G. A. Sawatzky, *Phys. Rev. Lett.* **80**, 4305 (1998).

- ²¹ I. I. Mazin, D. J. Singh, and C. Ambrosch-Draxl, Phys. Rev. B **59**, 411 (1999); I. I. Mazin, D. J. Singh, and C. Ambrosch-Draxl, J. Appl. Phys. **85**, 6220 (1999).
- ²² Horng-Tay Jeng, and G. Y. Guo, J. Appl. Phys. **92**, 951 (2002).
- ²³ J. Kuneš, P. Novák, P. M. Oppeneer, C. König, M. Fraune, U. Rüdiger, G. Güntherodt, C. Ambrosch-Draxl, Phys. Rev. B **65**, 165105 (2002).
- ²⁴ M. Komelj, C. Ederer and M. Fähnle, Phys. Rev. B **69**, 132409 (2004).
- ²⁵ A. Toropova, G. Kotlair, S. Y. Savrasov, and V. S. Oudovenko, Phys. Rev. B **71**, 172403 (2005).
- ²⁶ *Core Level Spectroscopies for Magnetic Phenomenon: Theory and Experiment*, edited by P. S. Bagus, G. Pacchioni, and F. Parmigiani (Plenum, New York, 1995).
- ²⁷ *Spin-Orbit Influenced Spectroscopies of Magnetic Solids*, edited by H. Ebert and G. Schütz, Lecture Notes in Physics Vol.466 (Springer-Verlag, Heidelberg, 1996).
- ²⁸ D. Weller, J. Stöhr, R. Nakajima, A. Carl, M. G. Samant, C. Chappert, R. Mégy, P. Beauvillain, P. Veillet, and G. A. Held, Phys. Rev. Lett. **75**, 3752 (1995).
- ²⁹ B. T. Thole, P. Carra, F. Sette, and G. van der Lann, Phys. Rev. Lett. **68**, 1943 (1992).
- ³⁰ P. Carra, B. T. Thole, M. Altarelli, and X. Wang, Phys. Rev. Lett. **70**, 694 (1993).
- ³¹ G. van der Lann, Phys. Rev. B **57**, 112 (1998).
- ³² C. T. Chen, Y. U. Idzerda, H.-J. Lin, N. V. Smith, G. Meigs, E. Chaban, G. H. Ho, E. Pellegrin, and F. Sette, Phys. Rev. Lett. **75**, 152 (1995).
- ³³ R. Wu, D. Wang, and A. J. Freeman, Phys. Rev. Lett. **71**, 3581 (1993); R. Wu and A. J. Freeman, *ibid.* **73**, 1994 (1994).
- ³⁴ E. Georing, A. Bayer, S. Gold, G. Schütz, M. Rabe, U. Rüdiger, and G. Güntherodt, Phys. Rev. Lett. **88**, 207203 (2002).
- ³⁵ E. Georing, A. Bayer, S. Gold, G. Schütz, M. Rabe, U. Rüdiger, and G. Güntherodt, Euro. Phys. Lett. **58**, 906 (2002).
- ³⁶ S. Gold, E. Goering, C. König, U. Rüdiger, G. Güntherodt, and G. Schütz, Phys. Rev. B **71**, 220404(R) (2005).
- ³⁷ G. van der Laan, J. Phys. C **9**, L259 (1997).
- ³⁸ H. Ebert, Rep. Prog. Phys. **59**, 1665 (1996).
- ³⁹ M. Alouani, J. M. Wills, and J. M. Wilkins, Phys. Rev. B **57**, 9502 (1998).
- ⁴⁰ C. Brouder and M. Hikam, Phys. Rev. B **43**, 3809 (1991); Ch. Brouder, M. Alouani, and K. H. Bennemann, *ibid.* **54**, 7334 (1996).
- ⁴¹ G. Y. Guo, Phys. Rev. B **57**, 10295 (1998).
- ⁴² A. Ankudinov and J. J. Rehr, Phys. Rev. B **56**, 1712 (1997).
- ⁴³ I. Galanakis, S. Ostanin, M. Alouani, H. Dreyssé, and J. M. Wills, Phys. Rev. B **61**, 599 (2000); I. Galanakis, S. Ostanin, M. Alouani, H. Dreyssé, and J. M. Wills, *ibid.* **61**, 4093 (2000).
- ⁴⁴ I. Galanakis, M. Alouani, and H. Dreyssé, Journal of Mag. and Mag. Mat. **242-245**, 27 (2002).
- ⁴⁵ G. van der Laan and B. T. Thole, Phys. Rev. B **43**, 13401 (1991).
- ⁴⁶ N. Baadji, M. Alouani, and H. Dreyssé (unpublished).
- ⁴⁷ J. M. Wills, O. Eriksson, M. Alouani and O. L. Price in *Electronic Structure and Physical Properties of Solids*, edited by H. Dreyssé (Springer, Berlin 2000).
- ⁴⁸ O. Jepsen and O. K. Andersen, Solid State Commun. **9**, 1763 (1971); G. Lehmann and M. Taut, Phys. Stat. Sol. **54**, 469 (1972).
- ⁴⁹ J. P. Perdew, K. Burke, and M. Ernzerhof, Phys. Rev. Lett. **77**, 3865 (1996).
- ⁵⁰ P. Porta, M. Marezio, J. P. Remeika, and P. D. Dernier, Mater. Res. Bull. **7**, 157 (1972).
- ⁵¹ T. Tsujioka, T. Mizokawa, J. Okamoto, A. Fujimori, M. Nohra, H. Takagi, K. Yamaura, and M. Takano, Phys. Rev. B **56**, R15509 (1997).
- ⁵² Ph. Mavropoulos, K. Sato, R. Zeller, P. H. Dederichs, V. Popescu, and H. Ebert, Phys. Rev. B **69**, 054424 (2004).
- ⁵³ G. Vaitheeswaran, V. Kanchana, and A. Delin, Appl. Phys. Lett. **86**, 032513 (2005).
- ⁵⁴ D. J. Huang, H. T. Jeng, C. F. Chang, G. Y. Guo, J. Chen, W. P. Wu, S. C. Chung, S. G. Shyu, C. C. Wu, H. J. Lin, and C. T. Chen, Phys. Rev. B **66**, 174440 (2002).
- ⁵⁵ E. Georing, Phil. Magazine B (2005) Accepted
- ⁵⁶ L. Spinu, H. Srikanth, A. Gupta, X. W. Li, and G. Xiao, Phys. Rev. B **62**, 8931 (2000).
- ⁵⁷ F. Y. Yang, C. L. Chein, E. F. Ferrari, X. W. Li, G. Xiao, and A. Gupta, Appl. Phys. Lett. **77**, 286 (2000).
- ⁵⁸ X. W. Li, A. Gupta, G. Xiao, Appl. Phys. Lett. **75**, 713 (1999).
- ⁵⁹ G. Miao, G. Xiao, A. Gupta, Phys. Rev. B **71**, 094418 (2005).
- ⁶⁰ E. Georing (Private communications).